Principles of Design of Fluid Transport Systems in Zoology

MICHAEL LABARBERA

Fluid transport systems mediate the transfer of materials both within an organism and between an organism and its environment. The architecture of fluid transport systems is determined by the small distances over which transfer processes are effective and by hydrodynamic and energetic constraints. All fluid transport systems within organisms exhibit one of two geometries, a simple tube interrupted by a planar transfer region or a branched network of vessels linking widely distributed transfer regions; each is determined by different morphogenetic processes. By exploiting the signal inherent in local shear stress on the vessel walls, animals have repeatedly evolved a complex branching hierarchy of vessels approximating a globally optimal system that minimizes the costs of the construction and maintenance of the fluid transport system.

THE DIVERSITY OF FORMS IN THE BIOLOGICAL WORLD IS dazzling, but there are limits to what may be molded by the evolutionary process. Some of these limitations [intrinsic constraints (*1*)] are inherent to biological systems: the limits to the maximum forces animals can produce (arising from the maximum stress that an actin-myosin–based force-producing organ can generate) or developmental constraints (*2, 3*) which limit the diversity of forms that evolution can produce from a given taxon. Extrinsic constraints (*1*) originate from the physical and mathematical structure of the universe in which organisms evolve (*4*). Examples range from the dependence of the strength of materials on the characteristics of molecular bonds to the manifold effects a change in size can exert on the biology of an organism (*5*), some arising from strictly geometrical considerations and others arising from changes in the relative magnitudes of physical forces such as surface tension, gravity, and viscosity (*6*).

To maintain their functional integrity, organisms must continually exchange materials with their environments and move materials within themselves. Such movement is almost invariably mediated by the convection of a fluid. In this article, I discuss the broad limitations that physical laws place on the structure of the systems which transport these fluids within organisms; external flows are a separate and much more complex topic. The advantage of approaching this subject from a physical perspective is that it allows one to perceive and understand common elements (that is, "design principles") in the structure of organisms. The architecture of these systems is not strongly influenced by the functional role that the fluid plays in the biology of the organism or by the nature of the circulation (that is, whether the fluid passes through the system only once or is continually recirculated).

The author is an associate professor in the Department of Organismal Biology and Anatomy at the University of Chicago, Chicago, IL 60637.

Transport Systems in Biology

Organisms transport fluids for two analogous but distinct reasons. The most common form of fluid transport system, an exchange system, is found in the vast majority of multicellular plants and animals; this system sidesteps the severe constraints that macroscopic distances place on the utility of diffusion. Such systems include classical circulatory systems, the unidirectional and tidal convective systems that move fluids to the respiratory structures of metazoans, xylem elements in tracheophytes, and the body cavities of a variety of coelomate and pseudocoelomate animals.

The second functional class of fluid transport system, a trophic system, is restricted to suspension-feeding animals, organisms that obtain nutrients by capturing organic particles that are in suspension in a fluid. Trophic fluid transport systems are rare only in comparison to the near universality of exchange fluid transport systems. For example, sponges, clams, brachiopods, a broad diversity of arthropods, ascidians, many fishes, and baleen whales all transport fluids through parts of their body, extracting suspended nutrients to support their metabolism and growth.

Why Must the Fluid Flow?

The most basic transport process in biology is diffusion, the net movement of molecules from regions of high concentration into regions of low concentration resulting from thermally driven random motion (*7*). On a cellular level, all transport processes ultimately involve diffusion. On small spatial scales, diffusion is rapid, reliable, and cheap. If a cell or organism merely binds or chemically transforms a molecule available in its environment, more molecules will be delivered by random thermal motion. The relevant aspects of diffusion are given by Fick's first law:

$$dS/dt = -D\ A\ dC/dx$$

where dS/dt is the rate of transport, A is the area through which diffusion occurs, dC/dx is the concentration gradient, and D is the diffusion coefficient of the substance.

The direct dependence of diffusion rates on the area through which diffusion occurs and the inverse dependence of these rates on distance imply that organisms (or parts of organisms) that depend on diffusion for exchange must be small or flat (to minimize the diffusion distance) and should have high surface-to-volume ratios

(to maximize the ratio of the area available for diffusion to the demand for materials). Small organisms or parts of organisms are thus well suited to use diffusion as a transport mechanism. However, with an increase in either organismal size or spatial scale, the situation becomes less favorable. Exchange transport systems have evolved to circumvent this problem.

The same problem arises for suspension feeding animals. The imperative for the maintenance of a flow of fluid past a suspension feeder's filtering structure is obvious: the vast majority of the biomass suspended in the oceans lies in the lower portion of the size spectrum of particles (*8*), and such particles have only limited motility. Many suspension feeders actively pump fluids past their filtering structures; in most of these animals, the vulnerable filters are hidden in their bodies, and fluids are moved to and away from the filters in trophic fluid transport systems. Particle capture in suspension feeders almost invariably involves direct contact between the particle and an element in the animal's filter; capture distances are on the order of the particle radius, 10^0 to 10^2 μm (*9*).

Despite the obvious differences in the central biological processes, the common constraint that links exchange and trophic fluid transport systems is the small physical distance over which the significant biological phenomenon is effective.

Principle 1: When a biologically relevant physical transfer process is limited to small spatial scales and local depletion of a necessary resource is threatened, bulk flow of a fluid will be utilized for long-distance transport of that resource.

The Architecture of Fluid Transport Systems

What characteristics should such fluid transport systems have? First, to avoid local exhaustion of the resource, the fluid must circulate (maintain dC/dx or supply particles). The pattern of circulation is not tightly constrained; although all recirculating transport systems are exchange systems and all trophic transport systems are through-flow systems, the converses of these statements are not true and no other simple generalities hold.

Second, distances must be minimized in the exchange sites (to keep the concentration gradients high or to allow particle capture).

Table 1. Systemic circulation of a 13-kg dog. Radii and lengths are average values; the area given is the aggregate cross-sectional area of the vessels. Note the increase in cross-sectional area and decrease in velocity in the transfer region (the capillaries). The capillaries are both small in radius and thin-walled; although the capillaries represent only about 0.07% of the length of the circuit, the blood spends about 4% of the circulation time there. A number of categories have been omitted here from the original tabulation (*90*); therefore, circulation times do not add to 100% (*91*).

Vessel	Radius (cm)	Number	Length (cm)	Area (cm^2)	Velocity (cm s^{-1})	Total circulation time (%)
Aorta	0.5	1	40	0.8	50	2
Large arteries	0.15	40	20	3.0	13.4	4
Terminal arteries	2.5×10^{-3}	1×10^6	0.1	19.6	2	0.1
Arterioles	1×10^{-3}	4×10^7	0.2	125	0.32	2
Capillaries	4×10^{-4}	1.2×10^9	0.1	600	0.07	4
Venules	1.5×10^{-3}	8×10^7	0.2	570	0.07	8
Terminal veins	6.5×10^{-3}	1×10^6	0.1	132	0.3	1
Main veins	0.12	600	10	27	1.48	19
Large veins	0.3	40	20	11	3.6	15
Vena cava	0.625	1	40	1.2	33.4	3

Table 2. Circulatory system of *Homo sapiens* (*92*). Numbers of vessels were calculated from average radii and aggregate areas given. Note the same features as in Table 1.

Vessel	Radius (cm)	Number	Area (cm^2)	Wall thickness (cm)
Aorta	1.25	1	4.5	0.2
Arteries	0.2	159	20	0.1
Arterioles	1.5×10^{-3}	5.7×10^7	400	2×10^{-3}
Capillaries	3×10^{-4}	1.6×10^{10}	4500	1×10^{-4}
Venules	1×10^{-3}	1.3×10^9	4000	2×10^{-4}
Veins	0.25	200	40	0.05
Vena cava	1.5	1	18	0.15

This requirement implies that the vessels carrying the fluid should be small (*10*). However, Poiseuille's law (*6*) implies that any such arrangement incurs a very high cost. For steady flow in a circular pipe

$$Q = \pi dPr^4/8L\mu$$

where Q is the volumetric flow rate, dP/L is the pressure drop per unit length of pipe, μ is the dynamic viscosity of the fluid, and r is the pipe radius. This equation is strictly applicable only in fully developed laminar flow [that is, Reynolds number (Re) (*11*) $< \approx 2000$ and ten diameters downstream of an entrance or branch], but it will serve as a useful guide. The implied restriction is severe. For constant Q, resistance to flow is proportional to r^{-4}; for a constant flow velocity, resistance is proportional to r^{-2}. In both cases, cost is directly proportional to the length of pipe.

Principle 2: Energetic considerations dictate that fluid transport systems utilize both large and small vessels; small vessels occur at exchange sites and are short, whereas all long-distance transport occurs in large vessels.

Although this might seem a straightforward criterion to implement, difficulties arise. Recall that diffusion occurs by the random motion of molecules; it takes a finite time to achieve equilibrium or any fraction thereof. To maximize the efficacy of the system, the fluid should spend a significant fraction of the circulation time at the exchange sites. Implementation of principle 2 in its simplest form, narrowing a large vessel down to a short, small vessel at the exchange site, would produce exactly the opposite result. Because the volume of fluid that enters the large vessel must also exit the small one, the lower cross-sectional area in the small vessel implies that the fluid must increase its speed. The fluid then spends the least time in the small vessel, because of both the increase in flow speed and the short length of the small vessel. Again, the solution is straightforward.

Principle 3: In fluid transport systems, the total cross-sectional area of the small vessels greatly exceeds that of the large vessels, so flow velocities in the small vessels are lower than those in the large vessels.

The exchange fluid transport systems in both plants and animals meet these three criteria. All systems consist of at least two distinct size classes of vessels. Exchange occurs in small vessels, which are both short and numerous. The aggregate cross-sectional area of the small vessels is always much greater than that of the large vessels; as a consequence, flow velocities are lowest in the smallest vessels. Representative data for mammals are given in Tables 1 and 2; see also (*12*).

The same constraints apply to trophic fluid transport systems (Table 3), albeit for slightly different reasons. Of the six particle capture mechanisms used by suspension feeders (*9*), one (inertial impaction) shows an increasing efficiency with increasing fluid velocity, but this mechanism has such a low efficiency for the low-

density organic particles and low Re typical of particle capture in suspension feeders that it is of minimal importance. Four of the particle capture mechanisms (*13*) become less efficient at higher velocities. All five of these capture mechanisms depend on adhesive interactions between the particle and filter; higher velocities increase the probability of particle loss. The efficiency of the remaining mechanism, sieving, is not directly dependent on fluid velocity, but sieving is rarely used by animals (*9*). There is a mild premium on higher velocities in the incurrent section of a trophic fluid transport system (before the filter) to prevent particle sedimentation on the walls, and a strong premium on high velocities in the excurrent section to ensure that the momentum of the water is high enough when it leaves the system to minimize the probability of refiltration. The trophic fluid transport systems of active suspension feeders fit the paradigm (Table 4); the total cross-sectional area of the filter greatly exceeds the cross-sectional area of the inflow and outflow pipes. For both trophic and exchange fluid transport systems, lower velocities in the transfer regions imply lower costs in moving the fluid.

The Geometries of Transfer Regions

Further analysis of the architecture of fluid transport systems depends on distinguishing between the two fundamentally different transfer-region geometries that occur in these systems. Planar transfer regions (Fig. 1), where the exchange sites are restricted to a single plane, occur in a wide variety of fluid transport systems. For example, particle capture in the trophic fluid transport systems of bivalved mollusks, brachiopods, and cephalochordates occurs on the ctenidia, lophophores, and gills, respectively; in all three, the transfer region is topologically a flat sheet. Respiratory exchange in the exchange transport systems of teleost fishes, cephalopod and gastropod mollusks, and brachyuran crabs occurs in the gills (termed ctenidia in the mollusks); in these cases also, the topology is that of a flat sheet.

Extensive folding of the transfer region often partially masks the fundamentally planar morphology. Folding increases the cross-sectional area through which the flow passes and thus decreases the average velocity of the fluid at the exchange sites. For any given size of vessel in the transfer region, this velocity reduction implies a lower cost in moving the fluid. This increase in cross-sectional area in the transfer region occurs both in systems with a low-velocity ciliary pump (bivalves, brachiopods, ascidians, cephalochordates, and gastropods) and in systems with a high-velocity muscular pump remote from the transfer region (fishes and cephalopods).

Typically, the planar transfer region partitions the fluid transport system into two sections, usually termed incurrent and excurrent, distinguished by whether the fluid has passed the exchange sites. The pipes in such a system rarely branch; the usual morphology consists of a small number (typically one) of incurrent openings and a small number (typically one or two) of large vessels leading to the excurrent opening or openings. All fluid transport systems with planar transfer regions have some feature that decreases the probability of recycling excurrent water [for example, down-current release of the excurrent stream in fishes and some ascidians (*14*); constriction of the excurrent opening to accelerate the fluid in bivalves, brachiopods, and cephalopods]. Although all fluid transport systems with planar transfer regions are through-flow systems, not all through-flow systems have planar transfer regions [for example, the fluid transport systems in sponges (trophic), bird lungs (exchange), and terrestrial plants (exchange) are all through-flow systems with nonplanar transfer regions].

In the second major geometry of transfer regions, distributed transfer regions (Fig. 2), the exchange sites are distributed in three-dimensional space, typically throughout the body of the organism. The most familiar examples are the circulatory systems of animals. In terrestrial plants, the exchange sites are the spongy mesophyll cells distributed through the body of the leaves, themselves distributed in three-dimensional space around the plant. A distributed geometry is rarer in trophic than in exchange fluid transport systems but does occur—the choanocytes, which act as both pump and filter in sponges, are found in choanocyte chambers scattered throughout

Table 3. Aggregate cross-sectional areas and water velocities in the trophic fluid transport system of a 100-μl segment of the sponge *Haliclona permollis* [abridged from (*93*)]. The collar slits of the choanocytes (the site of particle capture) are the transfer region; because the cross-sectional area is extremely high, the velocity is very low. The reduced cross-sectional area of the osculum accelerates the excurrent jet and helps reduce refiltration.

Site	Area (mm^2)	Velocity ($\mu m\ s^{-1}$)
Ostia	13.1	570
Inhalant canal apertures	4.3	1700
Prosodi	129	57
Prosopyles	89	83
Choanocytes		
Collar bases	1500	4.9
Collar slits	2400	3.1
Collar apertures	350	21
Apopyles	180	41
Exhalant canal apertures	1.3	5700
Osculum	0.14	5.13×10^4

Table 4. Cross-sectional areas and velocities in the trophic fluid transport systems of a variety of suspension-feeding marine invertebrates. "Incurrent" and "excurrent" are those regions of the fluid transport system upstream and downstream of the transfer region, respectively. For the mollusks and chordate, these regions are the incurrent and excurrent siphons; for the brachiopods, they are the lateral incurrent and median excurrent gapes. Note the increase in area and decrease in velocity in the transfer regions; in general, the fluid leaves the systems with a high velocity. For the mollusks, the area given for the transfer region is the total area of ostia in the ctenidium. For the brachiopods, velocities at the lophophore (the transfer region) were calculated from (*84*) on the assumption that stagger of the lophophore filaments yields an area open to the flow equivalent to the projected area of the lophophore.

Species	Cross-sectional area (cm^2)			Average velocity ($cm\ s^{-1}$)		
	Incurrent	Transfer region	Excurrent	Incurrent	Transfer region	Excurrent
			Mollusca			
*Mytilus edulis**	0.8	4.25	0.16	1.25	0.236	6.25
Crassostrea gigas†	0.85	78.2	2.43	3.48	0.038	1.22
			Brachiopoda			
Terebratalia transversa	0.970	11.340	0.293	0.31	0.027	1.03
Laqueus californianus	0.545	5.075	0.225	0.13	0.014	0.32
			Chordata			
Styela clava‡	0.503	25.3	0.196	1.51	0.03	3.87

*Data from (*85*) for an "average" animal 3.5 cm long pumping 1 $cm^3\ s^{-1}$. The velocity in the mantle cavity given in (*85*) is obviously in error; it assumes that the cross-sectional area in the mantle cavity perpendicular to the flow is equal to the area of the ctenidia [see (*86*)]. †Data from (*87*) for a 15-cm-long animal. A volumetric flow rate of 177.7 $cm^3\ s^{-1}$ was calculated, based on regressions in (*88*). The highest velocities occur in the incurrent siphon, contrary to the pattern generally seen in bivalves. ‡Data from (*89*) for a 0.412-g animal (dry weight). The transfer region is the mucus sheet overlying the gill bars in the pharynx.

the sponge. Because the transfer regions in systems with this geometry are widely dispersed, the fluid transport systems themselves must have a more complex geometry than in systems with planar transfer regions; in particular, they tend to have a hierarchy of sizes of vessels, each of which is joined to the whole at branch points in the system. What rules govern the architecture of this branching hierarchy? Assuming that (i) it costs energy to move the fluid; (ii) laminar, fully developed Poiseuille flow of a Newtonian fluid occurs throughout the system (Fig. 3A); (iii) there is some cost to building or maintaining the system (the vessels) and its contents (the fluid); and (iv) there is some function that maximizes return on the system for the costs of construction, maintenance, and operation, Murray (*15–17*) derived the following relation:

Principle 4 (Murray's Law): In an optimally designed system involving bulk laminar flow of a Newtonian fluid through pipes, at any branch point the radius of the parent vessel (r_0) cubed will equal the sum of the cubes of the radii of the daughter vessels (r_1, r_2, r_3, . . . r_n):

$$r_0^3 = r_1^3 + r_2^3 + \ldots + r_n^3$$

Murray's original derivation minimized the costs of forcing the fluid (blood) through the pipes (blood vessels) against the action of the fluid's viscosity and the costs of building and maintaining the system (blood and blood vessels). However, the latter cost may be replaced by any cost associated with the volume of the system as a whole (*18*). This relation holds only for laminar flow; for turbulent flow regimes, the exponent would be 2.33 rather than 3 (*18–20*).

Tests of Murray's Law

There has been some controversy over the validity of Murray's law (*18, 20, 21*), but it appears robust when appropriate tests are applied. Hutchins *et al.* (*22*) measured vessel diameters at 42 branch points in normal human left main coronary arteries; the mean exponent relating parent and daughter vessel radii was 3.2 (±0.25).

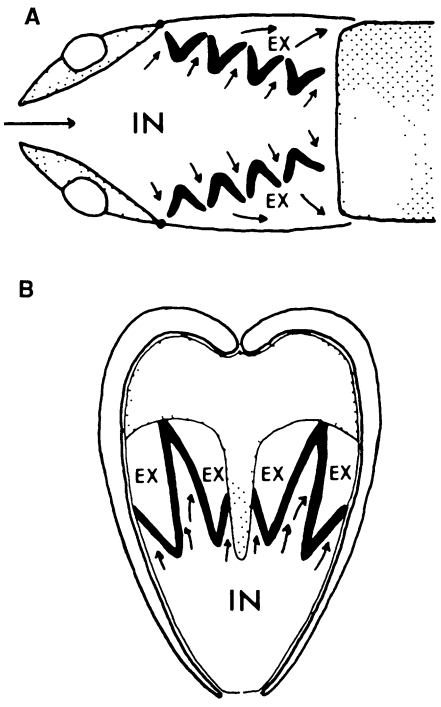

Fig. 1. Fluid transport systems with a planar geometry of the transfer regions. Direction of flow is indicated by arrows. The incurrent (IN) and excurrent (EX) parts of the systems are labeled; the transfer regions are indicated in solid black. (**A**) Schematic horizontal section through a generalized teleost fish, showing an exchange fluid transport system. Flow is driven by muscular action of the buccal floor and opercula; the transfer regions are the gills. (**B**) Schematic cross section through a generalized eulamellibranch bivalve mollusk. Although the transfer regions (the ctenidia) are involved in respiration, their primary function is particle capture; hence, this is a trophic fluid transport system. Water flow in both the incurrent and excurrent regions is primarily perpendicular to the plane of the drawing.

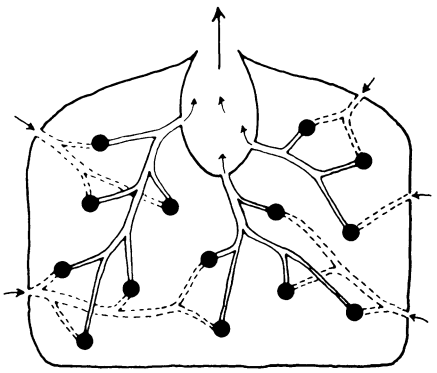

Fig. 2. A fluid transport system with distributed transfer regions (black), illustrating the branching hierarchy of the vessels. This highly schematized drawing of the trophic fluid transport system of a sponge shows the incurrent canals (dashed lines) and excurrent canals (solid lines) that carry water toward and away from, respectively, the choanocyte chambers. Flow directions are indicated by arrows.

Vessels from pathologic hearts yielded smaller values for the exponent, as did a heterogeneous grouping of other coronary arteries; none of these values were significantly different from a value of 3 (*23*). Zamir *et al.* (*24*) compared the dimensions of vessels at ~500 branch points in rat arterial systems to those predicted by Murray's law; agreement with theory appears to be good, but statistical measures were not given.

In a variation on this approach, LaBarbera and Boyajian (*25*) measured vessels (diameters from 89 to 502 μm) in the astrorhizal system of three species of Devonian stromatoporoids (an extinct group of sponges). The astrorhizae are usually interpreted as a network of excurrent canals (*26*). For each triplet of vessels at a dichotomous branch point, an expected parent vessel diameter was calculated from the daughter vessels' diameters, on the assumption that Murray's law was valid. Mean differences between observed and calculated parent vessel diameters for 361 branch points in five distinct astrorhizal complexes ranged from 0.6 to 5.8 μm (none significantly different from zero).

Murray's law implies that, at any level in the hierarchy of vessels, the sum of the cubed radii should yield a constant value (*16, 18*). The data presented here for mammalian circulatory systems (Table 5) and the fluid transport systems of four species of sponges (Tables 6 through 8) utilize this relation. Except for the choanocyte chambers and apopyles (discussed below), the vessels in sponges meet this rule within a factor of 3, excellent agreement considering that the values for vessel diameters and numbers are estimates from small samples of tissue. The data for mammalian circulatory systems fit the model less well; arterial and venous vessels yield different values, whereas values for the arterioles and capillaries differ markedly from those of both arterial and venous vessels.

This mode of analysis has a weakness, however. Any grouping of vessels, be it anatomical (the human and dog data in Table 5), functional (the sponge data in Tables 6 through 8), or obtained following various vessel ranking methods (*27–31*) (the hamster muscle in Table 5), necessarily groups vessels of different sizes into the same category. Calculation of a mean value for radius weights all vessels equally; the sum of the number of vessels times the mean radius cubed will equal the sum of the individual cubed radii only if the number of vessels is inversely proportional to the radius cubed. Precisely these arbitrary categorizations have been used in most studies on the architecture of the bronchial and circulatory systems (*32–38*).

A more direct test utilizes a relation implicit in Murray's law (*18*):

$$Q = kr^3$$

where r is the radius of the vessel and k is a constant. Mayrovitz and Roy (*39*) measured flow rates and radii in 160 vessels in the rat arteriolar circulation; vessel radii ranged from 3 to 54 μm. The

exponent of r that they derived was 3.01 (95% confidence interval = 2.86 to 3.14). This result was robust to the genotype of the rats and the vascular state; the mean exponent of six different treatments was 2.997 (±0.026). Kobari *et al.* (*40*), in a similar study of the flow in plial arteries (radius 10 to 100 μm) in cats, obtained an exponent of 2.98 (*41*).

The most common approach (*20, 21, 42, 43*) to testing the validity of Murray's law (and alternative optimization models) utilizes the dependence of branching angle at a branch point on the relative size of the daughter vessels. A number of alternative formulations of the relation are possible; all predict that daughter vessels with smaller radii should make steeper angles to the parent vessel. Analysis of branching angles has, in general, shown poor agreement with theoretical predictions. Zamir *et al.* (*24*) measured both diameters and angles of branches at 500 branch points in rat arterial systems; measured angles match theoretical predictions much less well than do diameter measurements from the same branch points. The angles predicted for different ratios of parent to daughter vessel diameters by different exponents are, in general, not greatly different (*43*); thus, this approach has not proved very useful. Zamir (*44*) contoured cost functions for angles of branching, using minimum power (minimum total drag) and combined minimum power and volume (Murray's law) models. Using data from a variety of mammalian arterial systems, Zamir found that, in all cases, Murray's law fit the observed angles better than did any alternative formulations. More importantly, in virtually all cases the overwhelming majority of the data points fell within the limits of a 5% cost above the optimum (*45*).

Although the available data are not definitive, it would appear that Murray's law is a useful approximation to the branching hierarchy of fluid transport systems with distributed transfer regions. This agreement is not an accident of geometry. The tracheal system in insects is superficially similar in architecture to the fluid transport systems discussed above, but bulk flow of air is either absent or limited to the largest vessels; O_2 is delivered to the tissues of the insect by diffusion. The vessels of insect tracheal systems follow the Σr^2 law expected for a diffusion-based system (*46, 47*) rather than the Σr^3 of Murray's law. Murray's law better describes the fluid transport system of sponges than the circulatory system of mammals. The bronchial system of mammals (*33*) matches less well than systems that involve the movement of liquids, probably because flow in the larger bronchi is turbulent (*48*) and bulk flow decreases in importance relative to diffusion in the smaller vessels. In these vessels, the assumptions underlying Murray's law are violated. A more general explanation for these discrepancies will be offered below.

Table 5. Exchange fluid transport systems in three mammals. For all three species, the Σr^3 (which should be constant by Murray's law) has been calculated. For *Homo sapiens*, values for Σr^2 (proportional to the area available for diffusion or inversely proportional to flow velocity) and Σr^4 (inversely proportional to resistance) are given for comparison. In general, Σr^3 yields relatively constant (but different) values for the arterial and venous systems, but values depart widely from those of both the arterial and venous systems in the smaller vessels (arterioles and capillaries). See text for explanation. For *Homo* and *Canis*, vessel radii are in centimeters; the Σr^3 values have been divided by 0.1 cm^3. For the hamster muscle, vessel radii are in micrometers; Σr^3 values have been divided by 1000 μm^3.

Vessel	Average radius	Number	Σr^2	Σr^3	Σr^4
		*Homo sapiens**			
Aorta	1.25	1	1.56	1.95	2.44
Arteries	0.2	159	6.36	1.27	0.25
Arterioles	3×10^{-3}	1.4×10^7	127.4	0.382	1.15×10^{-3}
Capillaries	6×10^{-4}	3.9×10^9	1432	0.860	5.16×10^{-4}
Venules	2×10^{-3}	3.2×10^8	1273	2.55	5.09×10^{-3}
Veins	0.25	200	12.9	3.18	0.80
Vena cava	1.5	1	2.25	3.38	5.06
		Canis familiaris†			
Aorta	0.5	1		1.25	
Large arteries	0.15	40		1.35	
Main arterial branches	0.05	600		0.75	
Terminal branches	0.03	1800		0.486	
Arterioles	1×10^{-3}	4×10^7		0.400	
Capillaries	4×10^{-4}	1.2×10^9		0.768	
Venules	1.5×10^{-3}	8×10^7		2.70	
Terminal veins	7.5×10^{-2}	1800		7.59	
Main venous branches	0.12	600		10.37	
Large veins	0.30	40		10.80	
Vena cava	0.625	1		1.53	
		Hamster cheek pouch retractor muscle arteriolar network‡			
Vessel order					
0	1.8	476		2.78	
1	2.85	144		3.33	
2	4.2	41		3.03	
3	7.6	12		5.27	
4	13.65	2		5.09	

*Data from (*92*); numbers of vessels calculated from aggregate areas and radii given. †Data from (*90, 94*); both attribute the basic data to Mall (*32*). ‡Data from (*37*). Vessel order was determined using Strahler ordering; centrifugal ordering produced no clear hierarchy of vessel sizes.

The Developmental Mechanism for Murray's Law Systems

How do biological systems of such wide phylogenetic distribution and differing functional roles all approach the architecture of a system of global optimality? What cues are available to organisms to use in generating such systems? In a Murray's law system, the shear stress (τ) on the walls of the vessels (49) is constant and equal everywhere throughout the system (*18*). If the endothelial cells lining blood vessels had a mechanism for measuring local shear stress and comparing that value to some set point, growth or shrinkage of vessels in which the shear stress departed from the set point would automatically produce a system that followed Murray's law (*50–53*)—local responses could produce a globally optimal system.

Evidence that endothelial cells in mammalian circulatory systems do indeed respond to local shear stress has accumulated in recent years (*54*); effects include flow-induced membrane K^+ currents at $\tau = 0.02$ to 1.70 N m^{-2} (*55*), protein secretion at arterial shear stresses ($\tau = 1.5$ to 2.5 N m^{-2}) but not at venous shear stresses ($\tau = 0.4$ N m^{-2}) (*56*), and membrane hyperpolarization that is a function of local shear stress up to 12.0 N m^{-2} (*57*). Long-term accommodations to surgically altered flow through the common carotid artery of dogs have been observed for both increased (up to fourfold) and decreased (as much as 96%) flow rates (*51*); over 6 to 8 months, changes in the vessels' diameters returned the wall shear stress to its original value (*58*). A similar regulation of wall shear stress occurs in the iliac artery of *Macaca fascicularis* (*59*); 6 months after surgical intervention increased the blood flow by a factor of 10, the artery had doubled in diameter, returning wall shear stress to its original value (~1.5 N m^{-2}). Langille and O'Donnell (*60*) demonstrated that wall shear stresses were regulated through diameter changes in the common carotid arteries of rabbits. A 70% flow reduction yielded a diameter reduction of 21% (raising shear stresses to 61% of their original value) in 2 weeks. Diameter change was not merely due to wall thickening or chronic contraction of the smooth muscle of the vessel wall and was critically dependent on the presence of the endothelium; removing the endothelium abolished the response (*61*). Interestingly, the response appeared to be local;

regions of the arterial wall where the endothelium was incompletely removed showed local diameter reduction (*60*).

A mechanism in which local shear stress determines the diameter of the vessel rationalizes the data for human and dog circulatory systems presented in Table 5. First, the shear rate set points for the arterial and venous endothelial cells apparently differ (*56, 62*); the mechanism determining this difference is unknown. Second, blood is a non-Newtonian fluid in which viscosity decreases when local shear rates increase; the effect is most pronounced in vessels with diameters smaller than about 300 μm (*31*). Those vessels in which Σr^3 departs most from the mean for the system, the arterioles and capillaries, are precisely those in which the effective viscosity of the blood should be most reduced. From the aorta through the capillaries, the wall shear stresses in the human systemic circulation range only from about 1.04 to 2.6 N m^{-2} (*52*); values for the venous circulation range from 0.14 to 0.63 N m^{-2} (*63*).

Approximate values for the shear rate (τ/μ) (*64*) in the vessels of two species of sponges (Tables 6 and 7) all lie within a factor of 3 for each sponge; here, too, vessel diameter may be determined by the response of the cells lining the vessels to local shear stress. Such a response would also account for the extreme discrepancies in the Σr^3 values for the choanocyte chambers and apopyles (excurrent openings of the choanocyte chambers) of the sponges in Tables 6 to 8. Flow in sponges is driven by the choanocytes' flagella; flow in the choanocyte chambers and apopyles is assuredly laminar ($Re \approx 10^{-3}$), but it is also assuredly not the parabolic velocity profile assumed in Poiseuille flow. In lieu of actual measurements of the velocity profile or local shear stress, these vessels cannot be included in the analysis. Do the cells lining the vessels in the fluid transport system of sponges respond to local shear stress? To date, only the endothelial cells in the vascular system of mammals have been investigated for sensitivity to shear stress.

A mechanism dependent on local shear stress clarifies some of the controversies. At every branch point in a system of branching pipes, the velocity profile will be temporarily altered. Near a branch point in large vessels, the medial sides of the daughter vessels will experience higher velocities and the lateral sides lower velocities than in fully developed flow (Fig. 3B) (*65–68*). Medial cells should respond as if they were in a vessel too small (shear stresses too high) and lateral cells as if they were in a vessel too large (shear stresses too low); unless the response is averaged around the vessel [see (*69*)], the result would be to alter branching angles to higher values than predicted from Murray's law. Because entrance or inlet length (distance to reestablish a parabolic velocity profile) is a function of Re, these effects should be greater in larger vessels (which have both a greater radius and flow velocity). This is the pattern seen in angles of branching in the human pulmonary artery (radii from 0.84 cm to 350 μm); smaller parent vessels better fit Murray's law than larger parent vessels (*21*). In small arterioles (radius 10 to 35 μm), the inverted pattern of velocity profile distortion (*70*) (Fig. 3C) implies that the angle of branching should decrease. When flows from two vessels merge (the venous system in mammals, the excurrent vessels in sponges, exhalation in the lungs), higher velocities occur near the

Table 6. The trophic fluid transport system of the sponge *Haliclona permollis*. Note that the Σr^3 is constant with a factor of 3 for all vessel types except the choanocyte chambers and apopyles (excurrent openings from the choanocyte chambers). Shear rate (τ/μ), which is proportional to shear stress on the vessel walls, follows a similar pattern (*64*). The excursion of values in the choanocyte chambers and apopyles is explained in the text. Data from (*93*) for a 100-μl mature segment. Radii are mean values (in micrometers); where means were not given, the midpoint of the range was used. Numbers of elements were calculated from the mean radius and the total cross-sectional areas given; the value for the osculum is the proportional fractional part of the whole. Σr^3 values have been divided by 10^8 μm^3.

Vessel	Radius	Number	Σr^3	τ/μ (s^{-1})
Ostia	10.3	3.93×10^4	0.429	222
Inhalant canal apertures	97.5	1.44×10^2	1.34	70
Prosodi	2.5	6.57×10^6	1.03	92
Prosopyles	1.5	1.26×10^7	0.425	222
Choanocyte chambers	15.5	1.20×10^6	44.7	
Apopyles	7.0	1.17×10^6	4.01	24
Exhalant canal apertures	187.5	11.77	0.776	122
Osculum	2100	0.01011	0.936	98

Table 7. The trophic fluid transport system of the sponge *Leucandra aspera*, after (*95*); vessel designations follow the original source. Values for Σr^3 and τ/μ (*64*) are relatively constant; the choanocyte chamber value is explained in the text. Average radius was calculated from aggregate cross-sectional areas and cited numbers of each element; the Σr^3 values have been divided by 10^9 μm^3. Conventions are as in Table 6.

Vessel	Radius	Number	Σr^3	τ/μ (s^{-1})
Afferent canals	40.6	8.1×10^4	5.43	123
Choanocyte chambers	27.3	2.25×10^6	46.5	
Efferent canals	123.7	5.2×10^3	9.84	68
Atrium	2585	1	17.3	39
Osculum	1405	1	2.77	242

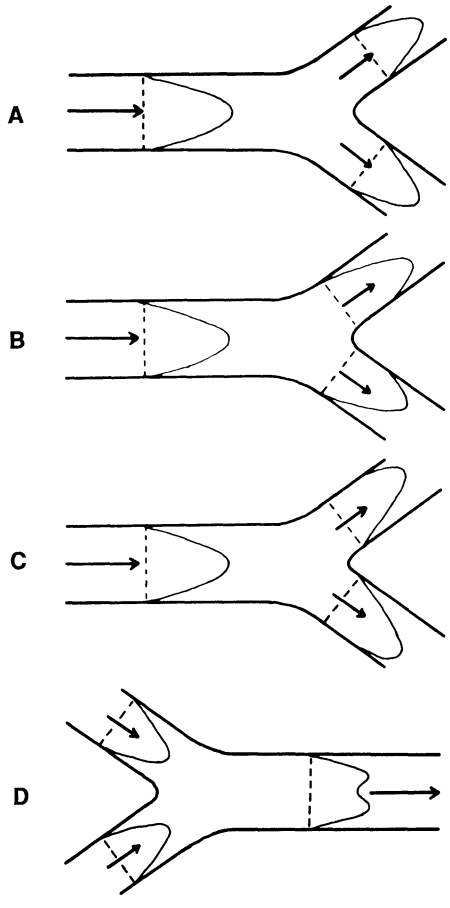

Fig. 3. Velocity profiles at branch points in vessels. In all cases, Re is assumed to be well below the critical value for turbulent flow (≈2000); arrows indicate the direction of flow. The flow in upstream vessels is assumed to be fully developed Poiseuille flow. The branching is assumed to be symmetrical; asymmetrical branching will distort the patterns shown but will not affect the qualitative relations. Local shear stress on the vessel wall will be proportional to the velocity gradient; the closer the point of maximum velocity lies to a wall, the higher the local shear stress. (**A**) The idealized flow pattern implicit in the derivation of Murray's law; in all vessels, the velocity profile is assumed to be fully developed. The maximum velocity is found at the center of the vessels, and the velocity profiles are parabolas; the maximum velocity is twice the average velocity. (**B**) Velocity profiles at branch points in large vessels ($100 < Re < 1500$). Because the flow divider at the branch point intersects the region of highest velocity in the parent vessel, the velocity profiles in the daughter vessels are skewed toward the median sides. (**C**) Velocity profiles at branch points in small vessels ($Re \approx 10^{-1}$ to 10^{-2}). The influence of the branch divider is felt upstream so that the velocity profiles in the daughter vessels are skewed toward the lateral walls. (**D**) Velocity profiles at a confluence of vessels. The profile of the merged flows shows a double peak with a minimum (but nonzero) velocity on the axis.

Table 8. The trophic fluid transport systems of the sponges *Haliclona panicea* and *Microciona prolifera*. The major deviations for Σr^3 occur in the choanocyte chambers and apopyles; see text. Calculations and conventions are as in Table 6.

Vessel	*Haliclona panicea*			*Microciona prolifera*		
	Radius	Number	Σr^3	Radius	Number	Σr^3
Ostia	8.95	6.56×10^4	0.470	6.7	1.28×10^5	0.384
Inhalant canal apertures	62.5	782	1.91	82.5	378.8	2.13
Prosodi	2.5	1.04×10^7	1.62	2.5	6.37×10^6	0.995
Prosopyles	1.5	9.76×10^6	0.329	2.5	5.55×10^6	0.861
Choanocyte chambers	12.5	1.8×10^6	35.2	20	1.00×10^6	80.0
Apopyles	6.5	1.54×10^6	4.23	4.5	1.13×10^6	1.03
Exhalant canal apertures	147.5	38.04	1.22	132.5	83.4	1.94
Osculum	600	0.06189	0.134	260	0.565	0.0993

walls and lower velocities in the center of the vessel (Fig. 3D) than in idealized Poiseuille flow (*66*). This is consistent with the generally higher values for Σr^3 in the venous system of mammals and the excurrent vessels of sponges (Tables 5 through 8).

Such secondary phenomena may also explain the generally better fit of data from circulatory systems than data from bronchial systems to Murray's law. On average, a bronchial tube is only 3.5 diameters long between branch points (*48*); a large part of these segments will be affected by the disturbed flow downstream of each branch (*71*). If shear stress is the signal used to generate these systems, vessel diameters are a poor test of optimality when the distance between branch points is small compared to the vessel diameter. In addition, because it is a tidal flow system, the local velocity profiles change shape when flow direction reverses (Fig. 3, B and D).

Derivations of optimal (minimal power loss) angles of branching that assume uniform flow throughout the vessels [for example, (*15, 19–21, 42, 43*)] ignore the true complexity of the hydrodynamics. Nevertheless, both flow visualization and pressure drop measurements (*67, 68*) indicate that a system modeled on Murray's law does surprisingly well in minimizing the flow disturbances at branch points. Matsuo *et al.* (*68*) determined the loss coefficient at branch points in a fluid transport system; the loss coefficient was a function of the diameter ratio of the vessels, the angle of branching, and the exponent relating volumetric flow rate to diameter. (The latter was varied from 2 to 3; Murray's law is predicated on a value of 3.) Despite the idealization of the flow implicit in Murray's law, an exponent of 3 yielded a lower loss coefficient for all realistic diameter ratios.

How General Are These Patterns?

The first three design principles hold for all fluid transport systems regardless of function or the geometry of the transfer region. Principle 4 (Murray's law) does not hold for fluid transport systems (again regardless of function) in which the transfer region is planar. Two factors appear to be at work in this case. First, dimensions of the vessels are not determined by local shear stress. Except in the transfer regions, the pipes are spaces (the oral cavity of fish, the mantle cavity of mollusks and brachiopods) with dimensions set by other determinants of morphogenesis. Second, total power loss in the system is directly minimized in that the diameters of all vessels except those in the transfer regions (which are short) are large and velocities in the transfer region are low. In these systems, there would appear to be no reason for natural selection to use the signal implicit in local shear stress.

Fluid transport systems with distributed transfer regions present more interesting cases. Here, by definition, a complex arrangement of pipes must distribute the fluid throughout the organism. Natural selection can easily exploit a local shear stress signal; response of cells to their immediate hydrodynamic environment will globally minimize the costs of building and running the fluid transport system. Such a mechanism is simple to implement and robust to changes in size, complexity, or activity during the development and growth of the organism.

Given the magnitude of organismal diversity, the available evidence on this point is meager. Closed circulatory systems have been described in cephalopod mollusks, annelids, and nemertine worms, but quantitative data on vessel radii or the relation between vessel radius and volumetric flow rate are lacking for animals other than vertebrates. The same is true for all animals with open circulatory systems (bivalve and gastropod mollusks and arthropods). Corrosion casts of the vascular systems of cephalopods (*72–74*), gastropods (*74, 75*), and decapod crustaceans (*76*) show the qualitative features expected. One would predict that vessels in open circulatory systems (which are lined with an endothelium) should follow Murray's law whereas the sinuses (which lack an endothelium) should not; quantitative data would be welcome. Despite the limitations of the available data, it strains credulity to believe that the only three systems for which quantitative data are available (sponges, stromatoporoids, and mammals) match the paradigm of Murray's law by chance, particularly given the phylogenetic distance between sponges and mammals. The stromatoporoid data imply that exploitation of a local shear stress signal to produce a near-optimal organism-spanning network of vessels evolved early in the Phanerozoic (by the Devonian at the latest).

The few obvious exceptions to Murray's law in organisms with demonstrated fluid transport systems and distributed transfer regions are more illuminating. Both the gastrovascular transport system in corals (Coelenterata) (*77*) and the coelomic circulatory system of crinoids (Echinodermata) (*78*) violate the rules of branching implied by Murray's law. In both, however, the vessels are completely lined with ciliated cells that drive the flow. Because shear between the fluid and the vessel is entirely developed along the cilium (*6, 79*), no local shear stress signal is available to the cells lining the vessels.

In seed plants, the hierarchy of vessels is strongly attenuated; most of the system (the stem and branches) consists of a parallel array of vessels (the xylem elements) of a limited size range (*80, 81*). Three factors oppose the evolution of a Murray's law system. First, the pipes consist of the cell walls of xylem elements; the vessels do not conduct fluids until the cell has died. Thus, no living tissue is present that can be used to detect local shear stress. Second, there may be an upper limit to the maximum diameter of vessel compatible with the tensile mechanism used by these plants to move water up the stem (*80*). Most cogent, however, is the irrelevance to the plant of the cost of moving fluids through the system; the pump is literally solar-powered (driven by evaporation from the leaves), and the plant

expends no metabolic energy in driving the flow. Even if a local shear stress signal were available to the plant, there would be no selective pressure to exploit it (*82*).

The widespread presence of systems carrying fluids in laminar flow that meet the four principles given above is the result of convergent evolution. The first three rules are dictated by the short spatial distances over which the transfer processes are effective, the high power requirement involved in forcing fluids through narrow spaces, and the necessity to limit flow velocities past the transfer regions. The solutions to these problems are evolutionarily simple and straightforward. The problem of arranging a branching hierarchy of pipes to deliver fluids to distributed transfer regions appears much more complex. Not only must the appropriate connections be made (*83*), but the system must be tuned to a global optimum if the costs of building and running the system are to be reasonable. That a simple signal, local shear stress, and local cellular responses to that signal can be used to construct a system that approximates minimal energetic expenditure is fortuitous, given the complex hydrodynamics implicit in such systems. The pathways open to evolution are indeed constrained, not because only one solution exists but because a simple local signal that will generally be available to cells in the vicinity of flowing fluids can be so easily utilized.

Comparative studies of fluid transport systems can be a powerful tool in analyzing how natural selection has exploited this opportunity. In the bronchial system of mammals, the confounding effects of diffusion in the lower pathways, turbulent flow in the larger bronchi, and the change in local velocity profiles during inhalation and exhalation should be separable. Study of the bronchial system of smaller mammals should eliminate the effects of turbulent flow because Re's are decreased. Quantitative data on the respiratory tree of holothurians (Echinodermata) should allow isolation of the effects of changing velocity profiles (resulting from tidal flow) from the effects of diffusion along the tubes. Whether fluid transport systems simply use the signal of local shear stress or actually optimize the system to minimize costs of construction and operation could also be determined by comparative studies. Flow in the large arteries of mammals of greater body size than humans is certainly turbulent; the exponent relating diameter to flow should be 2.33 rather than 3 (*19*) if these systems are truly optimized by natural selection.

REFERENCES AND NOTES

1. G. V. Lauder, *Paleobiology* 7, 430 (1981).
2. P. Alberch and E. A. Gale, *Evolution* **39**, 8 (1985).
3. R. A. Raff, *Dev. Biol.* **119**, 6 (1987).
4. R. M. Alexander, *Biol. J. Linn. Soc.* **26**, 345 (1985).
5. K. Schmidt-Nielsen, *Scaling: Why Is Animal Size So Important?* (Oxford Univ. Press, Oxford, 1984).
6. S. Vogel, *Life in Moving Fluids* (Williard Grant, Boston, 1981).
7. H. C. Berg, *Random Walks in Biology* (Princeton Univ. Press, Princeton, NJ, 1983).
8. J. Rodriguez and M. M. Mullin, *Limnol. Oceanogr.* **31**, 361 (1986).
9. M. LaBarbera, *Am. Zool.* **24**, 71 (1984).
10. Secondary considerations may reinforce this pattern. In animals that use cilia or flagella to drive the flow (for example, cilia on the respiratory ctenidia of gastropods or the suspension-feeding ctenidia of bivalves), momentum transfer between the cilia or flagella and the fluid is also a short-range phenomenon limited essentially to the length of the driving organelle.
11. Reynolds number is equal to $\rho rU/\mu$, where ρ is the density of the fluid, r is the radius of the vessel, U is the flow velocity, and μ is the dynamic viscosity of the fluid. It is equivalent to the ratio of the inertial to viscous forces in a flow situation (*6*).
12. M. LaBarbera and S. Vogel, *Am. Sci.* **70**, 54 (1982).
13. The particle capture mechanisms of direct interception, gravitational deposition, diffusive or motile-particle deposition, and scan and trap capture all become less efficient as local flow velocities increase. See (*9*) for a full description and discussion.
14. C. M. Young and L. F. Braithwaite, *Biol. Bull. Woods Hole, Mass.* **159**, 428 (1980).
15. C. D. Murray, *J. Gen. Physiol.* **9**, 835 (1926).
16. _____, *Proc. Natl. Acad. Sci. U.S.A.* **12**, 207 (1926).
17. Throughout the rest of this discussion I will use the phrase "Murray's law" as shorthand for an idealized model that simultaneously minimizes the cost of pumping the fluid and the total volume of the system.
18. T. F. Sherman, *J. Gen. Physiol.* **78**, 431 (1981).
19. H. B. M. Uylings, *Bull. Math. Biol.* **39**, 509 (1977).
20. A. Roy and M. J. Woldenberg, *ibid.* **44**, 349 (1982).
21. M. J. Woldenberg and K. Horsfield, *J. Theor. Biol.* **104**, 301 (1983).
22. G. M. Hutchins, M. M. Miner, J. K. Boitnott, *Circ. Res.* **38**, 572 (1976).
23. R. A. Groat [*Fed. Am. Soc. Exp. Biol. Proc.* 7, 45 (1948) (abstract)] reported an exponent of 2.6.
24. M. Zamir, S. M. Wrigley, B. L. Langille, *J. Gen. Physiol.* **81**, 325 (1983).
25. M. LaBarbera and G. E. Boyajian, in preparation.
26. G. E. Boyajian and M. LaBarbera, *Lethaia* **20**, 223 (1987).
27. Strahler ordering preserves the hierarchy of vessel sizes better than centrifugal ordering, but neither method is justifiable if the objective is to test some power law relation between levels in the branching hierarchy, whatever the presumed exponent. Objections to these vessel classification schemes have been raised on other grounds (*28–31*).
28. M. Zamir and H. Chee, *Blood Vessels* **24**, 76 (1987).
29. L. Koblinger and W. Hofmann, *Phys. Med. Biol.* **30**, 541 (1985).
30. _____, *Anat. Rec.* **221**, 533 (1988).
31. R. Skalak, N. Ozkaya, T. C. Skalak, *Annu. Rev. Fluid Mech.* **21**, 167 (1989).
32. J. P. Mall, *Abh. Math.-Phys. Koniglich Sach. Gessell. Wissen.* **14**, 151 (1888).
33. K. Horsfield and G. Cumming, *Bull. Math. Biophys.* **29**, 245 (1967).
34. K. Horsfield and A. Thurlbeck, *Bull. Math. Biol.* **43**, 681 (1981).
35. E. T. Engelson, T. C. Skalak, G. W. Schmid-Schonbein, *Microvasc. Res.* **30**, 29 (1985).
36. E. T. Engelson, G. W. Schmid-Schonbein, B. W. Zweifach, *ibid.* **31**, 356 (1986).
37. M. L. Ellsworth, A. Liu, B. Dawant, A. S. Popel, R. N. Pittman, *ibid.* **34**, 168 (1987).
38. A. G. Hudetz *et al.*, *J. Cereb. Blood Flow Metab.* 7, 342 (1987).
39. H. N. Mayrovitz and J. Roy, *Am. J. Physiol.* **245**, H1031 (1983).
40. M. Kobari *et al.*, *J. Cereb. Blood Flow Metabol.* **4**, 110 (1984).
41. N. Suwa *et al.* [*Tohoku J. Exp. Med.* **79**, 168 (1963)] took a similar approach in their analysis of the human circulatory system; their values for the exponent ranged from 2.51 to 2.87 (mean, ~2.7). However, they acknowledge that their procedure for producing vessel casts yielded differential dilation of vessels of different sizes; a post hoc correction was attempted, but the data must be considered suspect.
42. M. Zamir, *J. Theor. Biol.* **62**, 227 (1976).
43. M. J. Woldenberg, *ibid.* **122**, 187 (1986).
44. M. Zamir, *ibid.* **120**, 111 (1986).
45. A 5% cost variation to build and run the system represents about a 10% variation in vessel radius. In general, the total power cost is more sensitive to decreases in vessel radius than to increases. See (*19*) and T. F. Sherman *et al.* [*J. Theor. Biol.* **136**, 245 (1989)].
46. V. B. Wigglesworth, *Proc. R. Soc. London Ser. B* **106**, 229 (1930).
47. T. Weis-Fogh, *J. Exp. Biol.* **41**, 207 (1964).
48. T. J. Pedley, *Annu. Rev. Fluid Mech.* **9**, 229 (1977).
49. Shear stress is drag arising from the viscosity of the fluid. The shear stress in laminar flow is given by $\tau = \mu dU/dy$, where dU/dy is the velocity gradient perpendicular to the walls. In Poiseuille flow in cylindrical tubes, $\tau = 4\mu Q/\pi r^3$.
50. S. Rodbard, *Cardiology* **60**, 4 (1975).
51. A. Kamiya and T. Togawa, *Am. J. Physiol.* **239**, H14 (1980).
52. A. Kamiya, R. Bukhari, T. Togawa, *Bull. Math. Biol.* **46**, 127 (1984).
53. A. Kamiya, J. Ando, M. Shibata, H. Masuda, *Biorheology* **25**, 271 (1988).
54. P. F. Davies, *News Physiol. Sci.* **4**, 22 (1989).
55. S.-P. Olesen, D. E. Clapham, P. F. Davies, *Nature* **331**, 168 (1988).
56. S. L. Diamond, S. G. Eskin, L. V. McIntire, *Science* **243**, 1483 (1989).
57. M. Nakache and H. E. Gaub, *Proc. Natl. Acad. Sci. U.S.A.* **85**, 1841 (1988).
58. For increases in flow beyond 400%, regulation of wall shear stress through diameter change was incomplete but in the appropriate direction. Initiation of this regulatory response could be detected as early as 1 week after flow rates were altered.
59. C. K. Zarins *et al.*, *J. Vasc. Surg.* **5**, 413 (1987).
60. B. L. Langille and F. O'Donnell, *Science* **231**, 405 (1986).
61. These long-term responses should not be confused with the acute response of arteries and arterioles to changing flow effected by contraction of smooth muscle cells (again apparently mediated by a response of the endothelial cells to local shear stress); see, for example, P. M. Vanhoutte, *Hypertension* **13**, 658 (1989); J. A. Vita *et al.*, *J. Am. Coll. Cardiol.* **14**, 1193 (1989).
62. R. M. Zwolak, M. C. Adams, A. W. Clowes, *J. Vasc. Surg.* **5**, 126 (1987).
63. Zarins *et al.* (*59*) presented similar values. H. H. Lipowsky and B. W. Zweifach [*Microvasc. Res.* 7, 73 (1974)] calculated values for τ in the microvessels of cat mesentary that varied almost 50-fold for vessels with diameters from 7 to 46 μm. However, their analysis presumed that the viscosity of the blood was constant.
64. These shear rates were calculated on the assumption of Poiseuille flow in the vessels. One cannot derive actual values for shear stress without knowing the viscosity of the seawater (dependent on both temperature and salinity). However, because seawater is a Newtonian fluid, shear stress will be directly proportional to shear rate.
65. Secondary flows will also be established that will further complicate the picture (*31, 48, 66*). Flow streamlines for realistic models of arterial branch points are presented in (*67, 68*).
66. C. G. Caro, T. J. Pedley, R. C. Schroter, W. A. Seed, *The Mechanics of the Circulation* (Oxford Univ. Press, Oxford, 1978).
67. T. Karino and H. L. Goldsmith, *Biorheology* **22**, 87 (1985).
68. T. Matsuo, R. Okeda, F. Higashino, *ibid.* **26**, 799 (1989).
69. P. F. Davies, S.-P. Olesen, D. E. Clapham, E. M. Morrel, F. J. Schoen, *Hypertension* **11**, 563 (1988).
70. M. Sato and N. Ohshima, *Biorheology* **25**, 279 (1988).

71. Vogel (*6*) recommended allowing a minimum of 1 pipe diameter downstream of an entrance to a pipe to develop a recognizable approximation to a parabolic velocity profile; because the profile in the entrance is not uniform, distances here would be even greater. For full (99%) development of the profile, the entrance length is equal to 0.116 Re · *r*. J. K. B. Krijger *et al.* [*J. Biomech.* **22**, 1193 (1989)] found that velocity profiles did not return to a parabolic velocity distribution for 30 to 80 pipe diameters downstream of a confluence of vessels.
72. L. S. Smith, *J. Morphol.* **113**, 261 (1963).
73. J. Browning, *Zoomorphology Berl.* **96**, 243 (1980).
74. G. B. Bourne, J. R. Redmond, D. D. Jorgensen, *Physiol. Zool.* **63**, 140 (1990).
75. J. Voltzow, *Zoomorphology Berl.* **105**, 395 (1985).
76. B. R. McMahon and L. E. Burnett, *Physiol. Zool.* **63**, 35 (1990).
77. E. H. Gladfelter, *Biol. Bull. Woods Hole, Mass.* **165**, 619 (1983).
78. J. C. Grimmer and N. D. Holland, *Zoomorphology Berl.* **94**, 93 (1979).
79. J. R. Blake, N. Liron, G. K. Aldis, *J. Theor. Biol.* **98**, 127 (1982).
80. W. F. Pickard, *Prog. Biophys. Mol. Biol.* **37**, 181 (1981).
81. F. W. Ewers and J. B. Fisher, *Am. J. Bot.* **76**, 645 (1989).
82. Crustacea (Arthropoda) with dendrobrachiate or trichobrachiate gills [P. A. McLaughlin, in *The Biology of the Crustacea*, vol. 5, *Internal Anatomy and Physiological Regulation*, L. H. Mantel, Ed. (Academic Press, New York, 1983), pp. 1–52] have a distributed transfer region in which a Murray's law system has not evolved. The most common gill type in the decapod crustaceans, the phyllobranchiate gill, shows a typical planar transfer geometry. The exchange surface of dendrobrachiate and trichobrachiate gills is clearly distributed in three-dimensional space, but there is no evidence of division of the channels between the filaments into some hierarchy of branched vessels. This example may be akin to straining at gnats. Such a distributed gill geometry may be the only option for these animals that increases gill surface area over the phyllobrachiate condition and yet is still compatible with molting. On the other hand, here, too, no shear stress signal is available; the epidermal cells on the gills are covered by the cuticle.
83. The problem of how branching is controlled in these diverse systems has yet to be addressed.
84. M. LaBarbera, *J. Exp. Mar. Biol. Ecol.* **55**, 185 (1981).
85. C. B. Jorgensen *et al.*, *Mar. Ecol. Prog. Ser.* **34**, 69 (1986).
86. N. R. Silvester and M. A. Sleigh, *J. Mar. Biol. Assoc. U.K.* **64**, 859 (1984).
87. F. R. Bernard, *Biol. Bull. Woods Hole, Mass.* **146**, 1 (1974).
88. P. R. Walne, *J. Mar. Biol. Assoc. U.K.* **52**, 345 (1972).
89. H. U. Riisgard, *Mar. Ecol. Prog. Ser.* **47**, 129 (1988).
90. H. D. Green, in *Medical Physics*, O. Glasser, Ed. (Year Book, Chicago, 1950), vol. 2, pp. 228–251.
91. A. S. Iberall [*Math. Biosci.* **1**, 375 (1967)] criticized the vessel dimensions presented by Green (*90*), in particular the values for the aorta and large arteries, and presented alternative values based on averages. As explained above, such averages can hide the pattern to be studied. Some idea of the variation can be gathered from Iberall's figure 2, where the diameters of the largest arteries vary by a factor of 2.
92. W. F. Ganong, *Review of Medical Physiology* (Lange Medical, Los Altos, CA, 1975).
93. H. M. Reiswig, *J. Morphol.* **145**, 493 (1975).
94. A. C. Burton, *Physiology and Biophysics of the Circulation* (Year Book, Chicago, 1972).
95. G. P. Bidder, *Q. J. Microsc. Sci.* **67**, 293 (1923).
96. I thank A. Biewener, P. Davies, and S. Vogel for helpful comments on this manuscript. This work was supported in part by NSF grant BSR 84-06731.

In Situ Interfacial Mass Detection with Piezoelectric Transducers

MICHAEL D. WARD* AND DANIEL A. BUTTRY

The converse piezoelectric effect, in which an electric field applied across a piezoelectric material induces a stress in that material, has spurred many recent developments in mass measurement techniques. These methods commonly rely on the changes in the vibrational resonant frequency of piezoelectric quartz oscillators that result from changes in mass on the surface of the oscillator. The dependence of frequency on mass has been exploited extensively for mass measurements in vacuum or gas phase, for example, thickness monitors for thin-film preparation and sensors for chemical agents. Advances in piezoelectric methodology in the last decade now allow dynamic measurements of minute mass changes ($<10^{-9}$ grams per square centimeter) at surfaces, thin films, and electrode interfaces in liquid media as well. Mass measurements associated with a diverse collection of interfacial processes can be readily performed, including chemical and biological sensors, reactions catalyzed by enzymes immobilized on surfaces, electron transfer at and ion exchange in thin polymer films, and doping reactions of conducting polymers.

THE SIGNIFICANCE OF INTERFACIAL PROCESSES IN RESEARCH and commercial applications (such as sensors, electroplating, and corrosion) has stimulated the development of methodologies that probe interfacial processes and chemistry at surfaces and thin films. Advances in piezoelectric methods in the last decade now make possible in situ determination of minute mass changes that occur at thin films and surfaces under a variety of conditions, including liquid media. The low cost and procedural and conceptual simplicity of these methods portend broad development of commercial and research applications. In this article we discuss the fundamental properties, methodology, and examples of recent applications that highlight the versatility of these mass-sensing piezoelectric transducers.

M. D. Ward is in the Central Research & Development Department, E. I. duPont de Nemours and Co., Inc., P. O. Box 80328, Wilmington, DE 19880–0328. D. A. Buttry is in the Department of Chemistry, University of Wyoming, Laramie, WY 82071–3838.

*Present address: Department of Chemical Engineering and Materials Science, University of Minnesota, 421 Washington Avenue, S.E., Minneapolis, MN 55455.

Piezoelectricity

In 1880, Jacques and Pierre Curie discovered that a mechanical stress applied to the surfaces of various crystals, including quartz, rochelle salt ($NaKC_4H_4O_6 \cdot 4H_2O$), and tourmaline, afforded a corresponding electrical potential across the crystal whose magnitude was proportional to the applied stress (*1*). This behavior is referred to as the piezoelectric effect, which is derived from the